

On the deformations of an electroactive solid subject to a uniform electric field in an orthogonal rheometer

K. R. RAJAGOPAL¹⁾, A. WINEMAN²⁾, P. ALAGAPPAN³⁾

¹⁾ *Department of Mechanical Engineering, Texas A&M University, College Station, TX 77843, Texas, USA*

²⁾ *Department of Mechanical Engineering, University of Michigan, Ann Arbor, MI 48109, USA, e-mail: lardan@umich.edu (corresponding author)*

³⁾ *Department of Civil Engineering, Indian Institute of Technology, Madras, Chennai, 60036, India*

IN THIS SHORT PAPER, WE EXTEND THE SEMINAL STUDY by BERKER [4] of pseudo-planar flows that occur in an orthogonal rheometer, essentially two parallel disks rotating about non-coincident axes at the top and bottom, to the case of an electroactive elastic solid. We obtain the expression for the stress, which is a function of the deformation as well as the electric field, in an electroactive elastic solid using standard representation theorems. We show that in the case of elastic solids, pseudo-planar displacements can take place, with each layer $z = \text{constant}$ rotating about a distinct center of rotation. We determine the nature of the locus of the centers of rotation, which can take on profiles that are distinctly different, based on the nature of the electric field, the applied pressure gradient and the rotation of the top and bottom plates.

Key words: electroactive solid, orthogonal rheometer, pseudo-planar motion, rotation about non-coincident axes.



Copyright © 2025 The Authors.

Published by IPPT PAN. This is an open access article under the Creative Commons Attribution License CC BY 4.0 (<https://creativecommons.org/licenses/by/4.0/>).

1. Introduction

THE ORTHOGONAL RHEOMETER IS AN INSTRUMENT that can be used to determine the properties of both fluid-like and solid-like materials. It essentially consists of two parallel plates rotating with the same angular speed, but about distinct axes. The material undergoes a motion that is the superposition of shear and rotation, which in nonlinear fluids and solids invariably produces normal stresses, which are not necessarily the same, leading to normal stress differences. The flow in an orthogonal rheometer, and the more general problem of flow engendered due to the rotation of plates, with different angular speeds, have been subject to considerable scrutiny. The flow of a fluid above a disk due to its rotation and the flow of a fluid between two parallel disks due to their rotation about a common axis or about distinct axes have been studied assiduously

since the seminal study of VON KARMAN [1] in the case of the Navier–Stokes fluid for the flow above a single rotating disk of infinite radius using a similarity transformation that reduced the partial differential equations to a system of ordinary differential equation. This study of von Karman was followed by those of BATCHELOR [2] and STEWARTSON [3], who studied the flow that occurs due to the flow of a Navier–Stokes fluid between two infinite parallel disks rotating about a common axis, but with differing angular velocities. Their studies showed the richness of solutions that are possible for the problem under consideration, in that different types of solutions can manifest themselves, even in the case of the Navier–Stokes fluid, even if one were restricted to looking for axially symmetric solutions.

In marked contrast, in a remarkable study of the problem of flow between two infinite parallel plates rotating about a common axis, with the same angular velocity, BERKER [4] showed that if one were to give up the requirement of axial symmetry, then an infinity of solutions is possible to the problem, these solutions corresponding to different conditions in the lateral surface of the body of fluid at infinity. The form of the velocity field that Berker chose belongs to the class of “pseudo planar” motions that he had introduced (see BERKER [5]), fluid particles that lie in a plane parallel to the plates continuing to move on that plane, with no particle having a motion in the direction perpendicular to the plates. Such is the flow that occurs in the orthogonal rheometer, an instrument used to measure the properties of nonlinear (non-Newtonian) fluids and nonlinear solids.

The psuedo-planar motion that the body undergoes, discussed by Berker within the context of fluids, can be visualized in the following manner: a stack of infinitely thin long playing records, with a wire threaded through the holes at the center in a shape that admits each record to rotate rigidly, the top and bottom records being offset. The shape of the threaded wire represents the “locus of the centers of rotation”. While in the case of fluids, Berker is referring to the velocities of the infinitely thin discs, in our case we are considering the displacements.

In the case of non-Newtonian fluids, there have been numerous studies concerning the flow in an orthogonal rheometer wherein both the disks rotate with the same angular velocity, but about distinct axes (see MAXWELL and CHARTOFF [6], BIRD and HARRIS [7], BLYLER and KURTZ [8], KEARSLEY [9], GORDON and SCHOWALTER [10], GOLDSTEIN and SCHOWALTER [11], AHRENS and GOLDSTEIN [12], RAJAGOPAL [13], RAJAGOPAL and WINEMAN [14], RAJAGOPAL *et al.* [15], BOWER *et al.* [16], FUSI *et al.* [17], YANAMUNDRA *et al.* [18], and others). The flow and stability of a second grade fluid between two rotating plates, extending the analysis of BERKER [4] was carried out by RAJAGOPAL and GUPTA [19]. A discussion of many of the studies can be found in the review article by RAJAGOPAL [20].

RAJAGOPAL [21] showed that the flow that occurs in an orthogonal rheometer is a motion with a constant principal relative stretch history (see NOLL [22] for the definition of a motion with constant principal relative stretch history) which implies that the flow can be captured by knowing just the first three Rivlin–Ericksen tensors (see RIVLIN and ERICKSEN [23] for a definition of Rivlin–Ericksen tensors). It can be further shown that one needs only knowledge of the first two Rivlin–Ericksen tensors to determine the constitutive relation even for the most complicated Simple fluid (see NOLL [24, 25] for the definition of a simple fluid).

While most of the studies pertain to the flow of fluids in an orthogonal rheometer, the instrument can also be used to determine the properties of solids. RAJAGOPAL and WINEMAN [26] studied the deformation of the neo-Hookean and Mooney–Rivlin bodies subject to the deformation pertinent to that of a material deforming in an orthogonal rheometer while CARROLL and RAJAGOPAL [27] studied unsteady motions of neo-Hookean and Mooney–Rivlin bodies subject to the same deformation. These studies were followed later by investigations into the deformation of an elastic body with a non-convex stored energy potential by RAJAGOPAL and WINEMAN [28], and RAJAGOPAL, MASSOUDI and WINEMAN [29] addressed themselves to the deformation of granular materials, and GUPTA *et al.* [30] carried out experiments on the flow of granular materials within the confines of an orthogonal rheometer.

Our interest here is to study the deformation of an electroelastic solid within the confines of an orthogonal rheometer using the very simplified constitutive relation developed for such materials by RAJAGOPAL and WINEMAN [31] which treats the electric field as a given variable rather than having to determine it by solving the usual balance equations of mechanics in conjunction with Maxwell’s equation. The constitutive theory that stems from a more general viewpoint that considers the various fields such as the electric field, magnetic field, etc., can be found in RAJAGOPAL and RUZICKA [32, 33], and BUSTAMANTE and RAJAGOPAL [34, 35] developed constitutive relations for electroelastic solids wherein the underlying elastic body is more general than classical Cauchy elastic bodies, given by implicit constitutive relations between the stress and deformation gradient (see RAJAGOPAL [36, 37]). Recently, RAJAGOPAL and WINEMAN [38] have developed universal relations for shear and the triaxial extension of an electroelastic solid, generalizing their earlier work of such universal relations for elastic bodies [39].

The organization of the paper is as follows. In the next section we introduce the constitutive relation for the electroelastic body. In Section 3 we consider the electroelastic body subject to an electric field along a variety of directions and in the final section we determine the shape of the locus of the centers of rotation corresponding to the different applied electric fields.

2. Constitutive equation

There are two possible choices for the material symmetry group of the constitutive equation for an isotropic nonlinear elastic electroactive solid, namely the full orthogonal group or the proper orthogonal group. Representations for both are presented in [31]. This work restricts attention to isotropy described by the full orthogonal group for which the constitutive equation is:

$$(2.1) \quad \mathbf{T} = -p\mathbf{I} + \alpha_1 \mathbf{E} \otimes \mathbf{E} + \alpha_2 \mathbf{B} + \alpha_3 \mathbf{B}^{-1} + \alpha_4 (\mathbf{B}\mathbf{E} \otimes \mathbf{E} + \mathbf{E} \otimes \mathbf{B}\mathbf{E}) \\ + \alpha_5 (\mathbf{B}^{-1}\mathbf{E} \otimes \mathbf{E} + \mathbf{E} \otimes \mathbf{B}^{-1}\mathbf{E}),$$

where \mathbf{T} is the Cauchy stress, p is a scalar that arises from the assumption of incompressibility, \mathbf{B} is the left Cauchy–Green tensor, \mathbf{E} is the electric field vector and α_i are scalar coefficients, i.e. material properties, that are functions of the invariants,

$$(2.2) \quad \begin{aligned} I_1 &= \text{tr}(\mathbf{E} \otimes \mathbf{E}), & I_2 &= \text{tr}(\mathbf{B}), & I_3 &= \text{tr}(\mathbf{B}^{-1}), \\ I_4 &= \text{tr}(\mathbf{B}\mathbf{E} \otimes \mathbf{E}), & I_5 &= \text{tr}(\mathbf{B}^{-1}\mathbf{E} \otimes \mathbf{E}). \end{aligned}$$

3. Kinematics for an electroactive solid in an orthogonal rheometer

An orthogonal rheometer is a device consisting of two parallel plates a distance $2h$ apart within which, a solid or a fluid whose material properties we wish to determine, is placed (see Fig. 1). The plates are bonded to the surfaces of

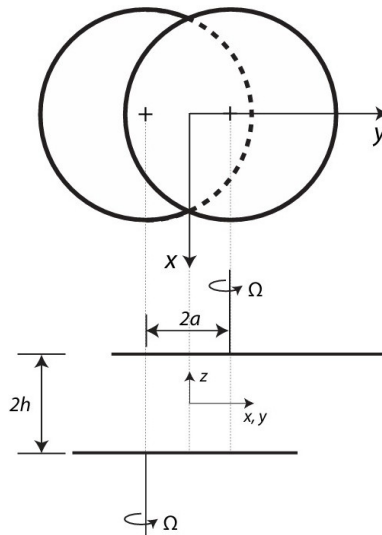


FIG. 1. Schematic drawing of an orthogonal rheometer.

the layer. They rotate about different axes that are normal to the plates, are parallel and are separated by a distance a . The rotation of the plates imposes a deformation of the layer in which each material particle undergoes a different shearing deformation. The forces and moments applied to the plates can be related to the shearing deformation and thereby provide information about the shearing properties of the medium. Moreover, if the material that is being tested is nonlinear, then the shearing motion causes normal forces to develop, and the measurement of these normal forces will aid in the determination of the material moduli that appear in the expression for such forces.

The orthogonal rheometer has been used to study the properties of various materials such as viscoelastic fluids [14, 16, 21] and granular materials [29]. In the present context, the layer is an ER solid, the plates act as electrodes and the orthogonal rheometer is used to study the interaction of the shearing deformation and an electric field.

Let the X - Y plane of a Cartesian coordinate system lie in the mid-surface between the parallel plates, and let the lower and upper plates coincide with planes $Z = -h$ and $Z = h$, respectively. The reference configuration for the electroactive solid is the layer between the plates before the plates are rotated and the electric field is applied. In this configuration the coordinates of a typical particle are (X, Y, Z) . The lower plate rotates through angle Ω about an axis through the point $(-a/2, 0, -h)$ and the upper plate rotates through angle Ω about an axis through the point $(a/2, 0, h)$. It is assumed that the plane at Z rotates about a point $(f(Z), g(Z), Z)$ and that these centers of rotation lie on a continuous curve connecting the points $(-a/2, 0, -h)$ and $(a/2, 0, h)$. Letting (x, y, z) denote the coordinates of a particle in the current configuration, the deformation of the layer is described by:

$$\begin{aligned} (3.1) \quad x &= (X - f(Z)) \cos \Omega - (Y - g(Z)) \sin \Omega + f(Z), \\ y &= (X - f(Z)) \sin \Omega + (Y - g(Z)) \cos \Omega + g(Z), \\ z &= Z. \end{aligned}$$

The motion (3.1) is a pseudo-planar motion, that is a motion in which particles in the $z = \text{constant}$ plane, move on the same plane, the motion however being different from one plane to another. Flows corresponding to such motions, namely pseudo-planar flows, were considered systematically by BERKER [4] who was able to establish explicit exact solutions in the case of the Navier–Stokes fluid. A generalization of the problem considered herein is that when the top and bottom plates are rotated by different angular displacements, this means that the problem is one of torsion superposed by shear. Such a deformation was first investigated by RAJAGOPAL and WINEMAN [28] within the context of neo-Hookean and Mooney–Rivlin materials. who determined a two parameter family

of exact solutions to the problem. When the angular displacement of both the top and bottom layers are the same, we recover the solution for the problem considered here, in the case of the neo-Hookean and Mooney–Rivlin materials. The motion was further generalized and studied, within the context of dynamics by CARROLL and RAJAGOPAL [27] for a variety of fluid models.

The deformation gradient associated with the motion is given by

$$(3.2) \quad \mathbf{F} = \begin{pmatrix} \cos \Omega & -\sin \Omega & f'(1 - \cos \Omega) + g' \sin \Omega \\ \sin \Omega & \cos \Omega & g'(1 - \cos \Omega) - f' \sin \Omega \\ 0 & 0 & 1 \end{pmatrix},$$

where, recalling (3.1) $(-)' = d(-)/dZ = d(-)/dz$.

The above deformation gradient (3.2) can be expressed as (see [28])

$$(3.3) \quad \mathbf{F} = \mathbf{Q}\mathbf{F}_1 = \mathbf{F}_2\mathbf{Q},$$

where \mathbf{Q} is a proper orthogonal tensor corresponding to rotation and \mathbf{F}_1 and \mathbf{F}_2 are deformation tensors corresponding to shear, i.e.:

$$(3.4) \quad (\mathbf{Q})_{XYZ} = \begin{pmatrix} \cos \Omega & -\sin \Omega & 0 \\ \sin \Omega & \cos \Omega & 0 \\ 0 & 0 & 1 \end{pmatrix},$$

$$(3.5) \quad (\mathbf{F}_1)_{XYZ} = \begin{pmatrix} 1 & 0 & g' \sin \Omega + f'(\cos \Omega - 1) \\ 0 & 1 & -f' \sin \Omega + g'(\cos \Omega - 1) \\ 0 & 0 & 1 \end{pmatrix}.$$

The tensor \mathbf{F}_1 can be shown to have the matrix representation:

$$(3.6) \quad (\mathbf{F}_1)_{\text{rotated}} = \begin{pmatrix} 1 & 0 & \hat{K} \\ 0 & 1 & 0 \\ 0 & 0 & 1 \end{pmatrix},$$

$$(3.7) \quad \hat{K} = \sqrt{2(f'^2 + g'^2)(1 - \cos \Omega)}$$

in a rotated co-ordinate system. One can similarly show that \mathbf{F}_2 is a linear transformation that corresponds to shear.

Thus, each layer undergoes a simple shear deformation but the amount of shear and its direction vary with Z and Ω . The inverse of the deformation gradient is

$$(3.8) \quad \mathbf{F}^{-1} = \begin{pmatrix} \cos \Omega & \sin \Omega & f'(1 - \cos \Omega) - g' \sin \Omega \\ -\sin \Omega & \cos \Omega & f' \sin \Omega + g'(1 - \cos \Omega) \\ 0 & 0 & 1 \end{pmatrix},$$

where \mathbf{F} , \mathbf{F}^{-1} and the terms defined through

$$(3.9) \quad \begin{aligned} A &= f'(1 - \cos \Omega) + g' \sin \Omega, & B &= -f' \sin \Omega + g'(1 - \cos \Omega), \\ C &= -f'(1 - \cos \Omega) - g' \sin \Omega, & D &= f' \sin \Omega - g'(1 - \cos \Omega), \\ \hat{D} &= 1 + (f'(1 - \cos \Omega) - g' \sin \Omega)^2 + (g'(1 - \cos \Omega) + f' \sin \Omega)^2 \\ &= 1 + [f'^2 + g'^2][2(1 - \cos \Omega)], \end{aligned}$$

the stress components are found to be:

$$(3.10) \quad T_{11} = -p + \alpha_1 E_1^2 + \alpha_2(1 + A^2) + \alpha_3 + 2\alpha_4[E_1^2(1 + A^2) + E_1 E_2 AB + E_1 E_3 A] + 2\alpha_5[E_1^2 + E_1 E_2 C],$$

$$(3.11) \quad T_{22} = -p + \alpha_1 E_2^2 + \alpha_2(1 + B^2) + \alpha_3 + 2\alpha_4[E_1 E_2 AB + E_2^2(1 + B^2) + E_2 E_3 B] + 2\alpha_5[E_2^2 + E_2 E_3 D],$$

$$(3.12) \quad T_{33} = -p + \alpha_1 E_3^2 + \alpha_2 + \alpha_3 \hat{D} + 2\alpha_4[E_1 E_3 + E_2 E_3 B + E_3^2] + 2\alpha_5[E_1 E_3 C + E_2 E_3 D + E_3^2 \hat{D}],$$

$$(3.13) \quad T_{12} = \alpha_1 E_1 E_2 + \alpha_2 AB + \alpha_4[E_1 E_2(2 + A^2 + B^2) + (E_1^2 + E_2^2)AB + E_2 E_3 A + E_1 E_3 B] + \alpha_5[2E_1 E_2 + E_2 E_3 C + E_1 E_3 D],$$

$$(3.14) \quad T_{13} = \alpha_1 E_1 E_3 + \alpha_2 A + \alpha_3 C + \alpha_4[E_1 E_3(2 + A^2) + (E_1^2 + E_3^2)A + E_2 E_3 AB + E_1 E_2 B] + \alpha_5[E_1 E_3(1 + \hat{D}) + (E_1^2 + E_3^2)C + E_1 E_2 D],$$

$$(3.15) \quad T_{23} = \alpha_1 E_2 E_3 + \alpha_2 B + \alpha_3 D + \alpha_4[E_2 E_3(2 + B^2) + (E_2^2 + E_3^2)B + E_1 E_3 AB + E_1 E_2 A] + \alpha_5[E_2 E_3(1 + \hat{D}) + (E_2^2 + E_3^2)D + E_1 E_2 C].$$

The invariants are:

$$(3.16) \quad \begin{aligned} I_1 &= E_1^2 + E_2^2 + E_3^2, & I_2 &= 3 + A^2 + B^2, & I_3 &= 2 + \hat{D}, \\ I_4 &= E_1^2(1 + A^2) + E_2^2(1 + B^2) + E_3^2 + 2E_1 E_2 AB + 2E_1 E_3 A + 2E_2 E_3 B, \\ I_5 &= E_1^2 + E_2^2 + E_3^2 \hat{D}^2 + 2E_1 E_3 C + 2E_2 E_3 D. \end{aligned}$$

On writing the stress tensor in the form $\mathbf{T} = -p\mathbf{I} + \hat{\mathbf{T}}(z)$, the equilibrium equations, in the absence of body forces, reduce to:

$$(3.17) \quad -\frac{\partial p}{\partial x} + \frac{d\hat{T}_{13}}{dz} = 0, \quad -\frac{\partial p}{\partial y} + \frac{d\hat{T}_{23}}{dz} = 0, \quad -\frac{\partial p}{\partial z} + \frac{d\hat{T}_{33}}{dz} = 0.$$

Cross differentiation to eliminate p gives:

$$(3.18) \quad \frac{d^2 \hat{T}_{13}}{dz^2} = 0, \quad \frac{d^2 \hat{T}_{23}}{dz^2} = 0.$$

Thus,

$$(3.19) \quad T_{13} = \hat{T}_{13} = \beta_1 + \beta_2 z, \quad T_{23} = \hat{T}_{23} = \gamma_1 + \gamma_2 z.$$

4. Deformations associated with various electric fields

4.1. $E_1 = E_2 = 0, E_3 \neq 0$

In this special case, the electric field vector is perpendicular to the plates and the layer. The relevant stress components reduce to the form:

$$(4.1) \quad \begin{aligned} T_{13} &= [f'(1 - \cos \Omega) + g' \sin \Omega]K, \\ T_{23} &= [-f' \sin \Omega + g'(1 - \cos \Omega)]K, \\ K &= \alpha_2 - \alpha_3 + (\alpha_4 - \alpha_5)E_3^2. \end{aligned}$$

Let it be assumed that the scalars α_i are constants so that K is independent of z . Then, after substituting the stresses in (4.1) into (3.19), the system can be integrated to give two equations for $f(z)$ and $g(z)$:

$$(4.2) \quad \begin{aligned} (f(1 - \cos \Omega) + g \sin \Omega)K &= \beta_0 + \beta_1 z + \beta_2 \frac{h^2}{2}, \\ (-f \sin \Omega + g(1 - \cos \Omega))K &= \gamma_0 + \gamma_1 z + \gamma_2 \frac{h^2}{2}. \end{aligned}$$

The boundary conditions on f and g , determined by the intersections of the axes of rotation with the lower and upper plates, are:

$$(4.3) \quad \text{lower: } f(-h) = -\frac{a}{2}, \quad g(-h) = 0, \quad \text{upper: } f(h) = \frac{a}{2}, \quad g(h) = 0.$$

On applying these boundary conditions, Eqs. (4.2) become:

$$(4.4) \quad \begin{aligned} (f(1 - \cos \Omega) + g \sin \Omega)K &= \frac{a}{2h}(1 - \cos \Omega)Kz + \frac{\beta_2}{2}(z^2 - h^2), \\ (-f \sin \Omega + g(1 - \cos \Omega))K &= -\frac{a}{2h} \sin \Omega Kz + \frac{\gamma_2}{2}(z^2 - h^2), \end{aligned}$$

whose solution for f and g is:

$$(4.5) \quad \begin{aligned} f(z)((1 - \cos \Omega)^2 + \sin^2 \Omega)K &= \frac{a}{2h}((1 - \cos \Omega)^2 + \sin^2 \Omega)Kz + \frac{z^2 - h^2}{2}(\beta_2(1 - \cos \Omega) - \gamma_2 \sin \Omega), \\ g(z)((1 - \cos \Omega)^2 + \sin^2 \Omega)K &= \frac{z^2 - h^2}{2}(\beta_2 \sin \Omega + \gamma_2(1 - \cos \Omega)). \end{aligned}$$

Two integration constants, β_2 and γ_2 , remain to be determined.

Since

$$(4.6) \quad dp = \frac{\partial p}{\partial x} dx + \frac{\partial p}{\partial y} dy + \frac{\partial p}{\partial z} dz,$$

it follows from (3.14)–(3.16), that

$$(4.7) \quad p = (\beta_2 x + \gamma_2 y) + \int \hat{T}_{33} dz + \tilde{C},$$

where \tilde{C} is a constant and $\hat{\mathbf{T}} = \mathbf{T} + p\mathbf{I}$.

We notice that the constants β_2 and γ_2 appear in the Eq. (4.7) for the pressure field, and if they are non-zero, it implies a pressure gradient along the x and y directions which are associated with deformation akin to the Poiseuille flows in fluids. We see later that it follows from (3.19) and (4.5) that if the shear stresses are to be the same on the upper and lower plates, then β_2 and γ_2 are zero, and vice-versa. The terms $\beta_2 x$ and $\gamma_2 y$ denote that there is a Poiseuille like flow due to the pressure gradient along these directions due to the forces at the edges of the plates. If there is no such pressure gradient, that is, if β_2 and γ_2 are both zero, then, the expressions in (4.5) reduce to:

$$(4.8) \quad f(z) = \frac{a}{2h} z, \quad g(z) = 0,$$

and the locus of the centers of rotation will be a straight line (see Fig. 3). However, if β_2 and γ_2 are not zero, then the locus of the center of rotation will not be a straight line and will be curved (see Fig. 2).

According to (3.7), the shear in the material elements in each layer is

$$(4.9) \quad \hat{K} = \sqrt{\frac{a}{h}(1 - \cos \Omega)}.$$

The shear is independent of the layer, the material properties and E_3 depend only on the plate separation h , the rotation axis spacing a and the plate rotation Ω . Furthermore, the locus of the centers of rotation of the surfaces of the layer is a straight line that lies in the x - z plane and does not vary with material properties or E_3 . On the other hand, if the forces on the plates are found to be different, then, according to (4.5), the shear at a material particle depends on the material properties and E_3 and its location z . The locus of the centers of rotation is a curve passing out of the x - z plane and whose shape varies with both the material and E_3 .

4.2. $E_1 \neq 0$, $E_2 \neq 0$, $E_3 = 0$

Using the notation in (3.9), the relevant stresses become:

$$(4.10) \quad \begin{aligned} T_{13} &= \alpha_2 A + \alpha_3 C + \alpha_4 (E_1^2 A + E_1 E_2 B) + \alpha_5 (E_1^2 C + E_1 E_2 D), \\ T_{23} &= \alpha_2 B + \alpha_3 D + \alpha_4 (E_1 E_2 A + E_2^2 B) + \alpha_5 (E_1 E_2 C + E_2^2 D). \end{aligned}$$

Now, with the expressions for A, B, C, D in (3.9) the stresses can be written directly in terms of f' and g' ,

$$(4.11) \quad \begin{aligned} T_{13} &= f'[K_1(1 - \cos \Omega) - K_{12} \sin \Omega] + g'[K_1 \sin \Omega + K_{12}(1 - \cos \Omega)], \\ T_{23} &= f'[K_{12}(1 - \cos \Omega) - K_2 \sin \Omega] + g'[K_{12} \sin \Omega + K_2(1 - \cos \Omega)], \end{aligned}$$

in which

$$(4.12) \quad \begin{aligned} K_1 &= \alpha_2 - \alpha_3 + E_1^2(\alpha_4 - \alpha_5), & K_{12} &= E_1 E_2(\alpha_4 - \alpha_5), \\ K_2 &= \alpha_2 - \alpha_3 + E_2^2(\alpha_4 - \alpha_5). \end{aligned}$$

Let it again be assumed that the scalars α_i are constants so that K_1, K_2, K_{12} are independent of z . Then, after substituting the stresses in (4.11) into (3.19), the system can be integrated to give two equations for $f(z)$ and $g(z)$,

$$(4.13) \quad \begin{aligned} f[K_1(1 - \cos \Omega) - K_{12} \sin \Omega] + g[K_1 \sin \Omega + K_{12}(1 - \cos \Omega)] &= \beta_0 + \beta_1 z + \beta_2 \frac{z^2}{2}, \\ f[K_{12}(1 - \cos \Omega) - K_2 \sin \Omega] + g[K_{12} \sin \Omega + K_2(1 - \cos \Omega)] &= \gamma_0 + \gamma_1 z + \gamma_2 \frac{z^2}{2}. \end{aligned}$$

After applying the boundary conditions, (4.13) become:

$$(4.14) \quad \begin{aligned} f[K_1(1 - \cos \Omega) - K_{12} \sin \Omega] + g[K_1 \sin \Omega + K_{12}(1 - \cos \Omega)] &= \frac{a}{2h} [K_1(1 - \cos \Omega) - K_{12} \sin \Omega]z + \frac{\beta_2}{2}(z^2 - h^2), \\ f[K_{12}(1 - \cos \Omega) - K_2 \sin \Omega] + g[K_{12} \sin \Omega + K_2(1 - \cos \Omega)] &= \frac{a}{2h} [K_{12}(1 - \cos \Omega) - K_2 \sin \Omega]z + \frac{\gamma_2}{2}(z^2 - h^2). \end{aligned}$$

Once again, depending on the structure of the pressure field, we can either have the locus of the centers of rotation as a straight line or a curve joining the centers of rotation on the top and bottom plates. The manner in which the locus of the centers of rotation changes with E_1 , with $E_2 = E_3 = 0$ is provided in Fig. 6, while the manner it changes with E_2 , $E_1 = E_3 = 0$ is portrayed in Fig. 7.

4.3. $E_2 = 0$, $E_1 \neq 0$, $E_3 \neq 0$

In this case it is intended that the electric field be normal to the plates but ends up having a component along the X -axis. Using the notation in (3.9), the relevant stresses become:

$$(4.15) \quad \begin{aligned} T_{13} &= (\alpha_1 + 2\alpha_4 + \alpha_5)E_1 E_3 + (\alpha_2 + (E_1^2 + E_3^2)\alpha_4)A \\ &\quad + (\alpha_3 + (E_1^2 + E_3^2)\alpha_5)A + E_1 E_3(\alpha_4 A^2 + \alpha_5 \hat{D}), \\ T_{23} &= (\alpha_2 + E_3^2 \alpha_4)B + (\alpha_3 + E_3^2 \alpha_5)D + E_1 E_3 \alpha_4 AB. \end{aligned}$$

Let these be substituted in (3.19) and use (3.9). This gives two coupled nonlinear equations for f' and g' . Even in the special case when the α_i are constants, it appears that analytical solutions for f' and g' cannot readily be established and they must be determined numerically. Our remarks in the previous section with regard to how the structure of the pressure affects the locus of centers of rotation apply once again.

5. Numerical example

We now determine how the functions $f(z)$ and $g(z)$, and hence the shape of the locus of the centers of rotation, defined by $(f(z), g(z), z)$, are affected by the angle of rotation and the electric field. In order to verify that our numerical scheme is valid, we tested the case when the electric field $E_1 = E_2 = E_3 = 0$, when β_2 and γ_2 are zero (that is, when the pressure gradients in the X and Y directions are absent), the top and bottom surfaces being rotated with the same angular displacement Ω about the points $(0, 0, -h)$ and $(0, 0, h)$ and $a = 0$ (corresponding to the plates rotating about the same axis), respectively. In this case we find that both $f(z)$ and $g(z)$ are constant and the solution is a rigid body rotation. We also find $f(z)$ and $g(z)$, once again when $a = 0$, β_2 and γ_2 are zero, and when the component of the electric field along the z -direction is not zero. As can be expected, since the electric field is along the axis of rotation, we once again find that $f(z)$ and $g(z)$ are constant. Figures showing this are omitted for the sake of brevity of the presentation. Next we consider the case when $a = 0$, but β_2 and γ_2 are non-zero (that is, they are pressure gradients present in both the X and Y directions). We see parabolic profiles associated with the deformation, as might be expected. This is depicted in Fig. 2.

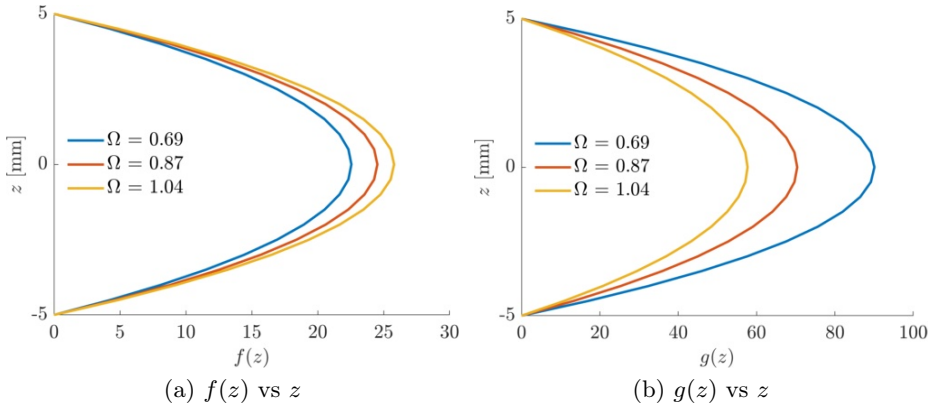


FIG. 2. Parameters $a = 0$, $h = 5$ mm, $\alpha_2 = \alpha_4 = 2$, $\alpha_3 = \alpha_5 = 1$, $\beta_2 = -10$, $\gamma_2 = -1$, $E_1 = E_2 = 0$, $E_3 = 1$.

When $a \neq 0$ (that is, when the plates are rotating about distinct axes), β_2 and γ_2 are zero (no pressure gradients in the X and Y directions), and the electric field is also zero, we see that $f(z)$ is a straight line that joins the centers of rotation of the top and bottom plates and $g(z)$ is a constant (see Fig. 3). Next, when there is no pressure gradient (β_2 and γ_2 are zero), but the electric field is purely along the z -axis, we once again find that the locus of centers of rotation is a straight line joining the centers of rotation of the top and bottom plates. This is again to be expected as the electric field is perpendicular to the plates and does not have an effect on the locus of the centers of rotation, the locus being completely determined by the displacement due to shear (recall the earlier discussion that showed that the deformation being considered is made up of a shear and a rotation). This is depicted in Fig. 4. Figure 5 portrays the situation when

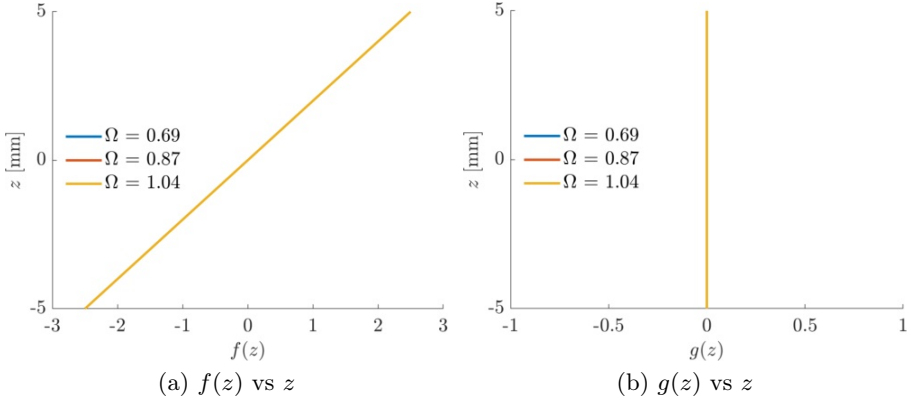


FIG. 3. Parameters $a = 5$ mm, $h = 5$ mm, $\alpha_2 = \alpha_4 = 2$, $\alpha_3 = \alpha_5 = 1$, $\beta_2 = 0$, $\gamma_2 = 0$, $E_1 = E_2 = 0$, $E_3 = 0$.

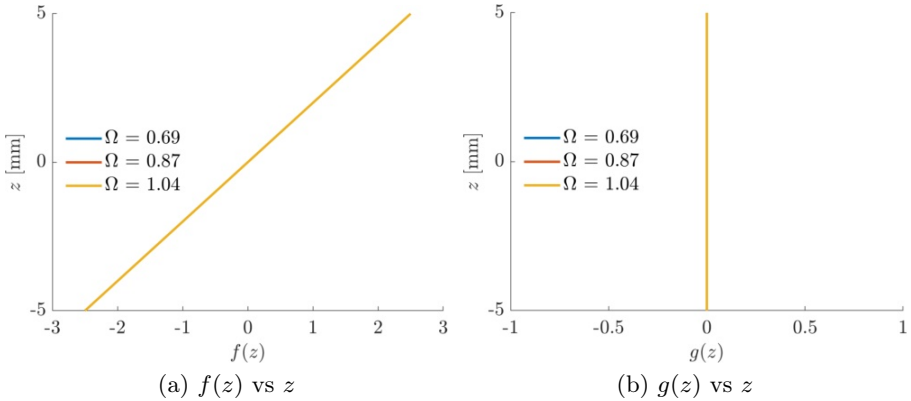


FIG. 4. Parameters $a = 5$ mm, $h = 5$ mm, $\alpha_2 = \alpha_4 = 2$, $\alpha_3 = \alpha_5 = 1$, $\beta_2 = 0$, $\gamma_2 = 0$, $E_1 = E_2 = 0$, $E_3 = 1$.

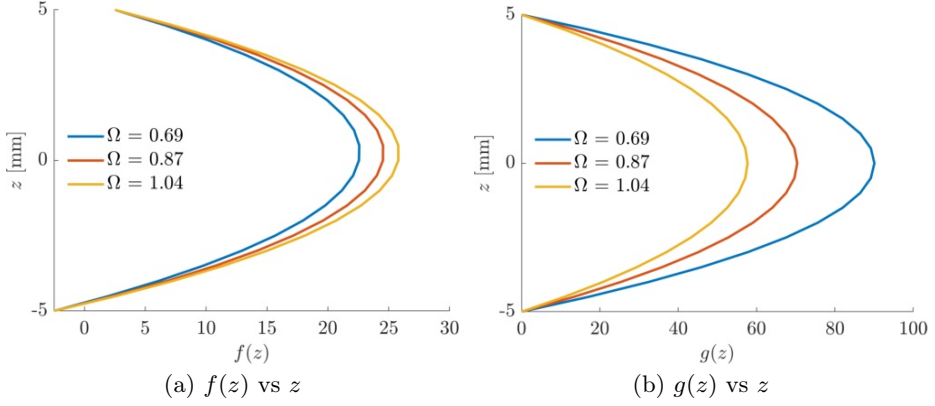


FIG. 5. Parameters $a = 5$ mm, $h = 5$ mm, $\alpha_2 = \alpha_4 = 2$, $\alpha_3 = \alpha_5 = 1$, $\beta_2 = -10$, $\gamma_2 = -1$, $E_1 = E_2 = 0$, $E_3 = 1$.

$a \neq 0$, β_2 and γ_2 are non-zero, while $E_3 \neq 0$, but E_1 and E_2 are zero. In this case, we find that the locus of the centers of rotation has a skewed parabolic profile due to the shearing associated with the initial offset of the plates to which the deformation due to the pressure gradient that would be parabolic, is suppressed. Figures 6–8 depict the variation of $f(z)$ versus z and $g(z)$ versus z , for different values of the electric field and the pressure gradients. All of them essentially have the skewed parabolic profile that is a consequence of the Poiseuille type flow superposed on the shearing due to the plates rotating about non-coincident axes.

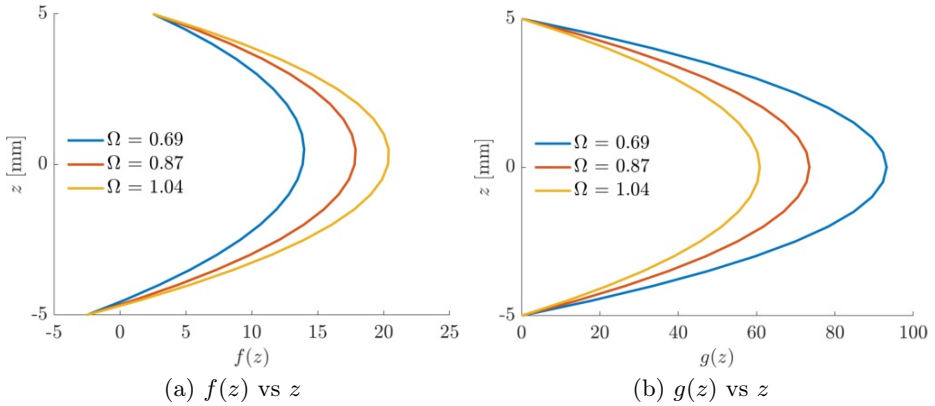


FIG. 6. Parameters $a = 5$ mm, $h = 5$ mm, $\alpha_2 = \alpha_4 = 2$, $\alpha_3 = \alpha_5 = 1$, $\beta_2 = -10$, $\gamma_2 = -1$, $E_1 = 1$, $E_2 = 0$, $E_3 = 0$.

A few important caveats are in order. The material parameters that have been chosen are arbitrary as there is no experimental determination that has been

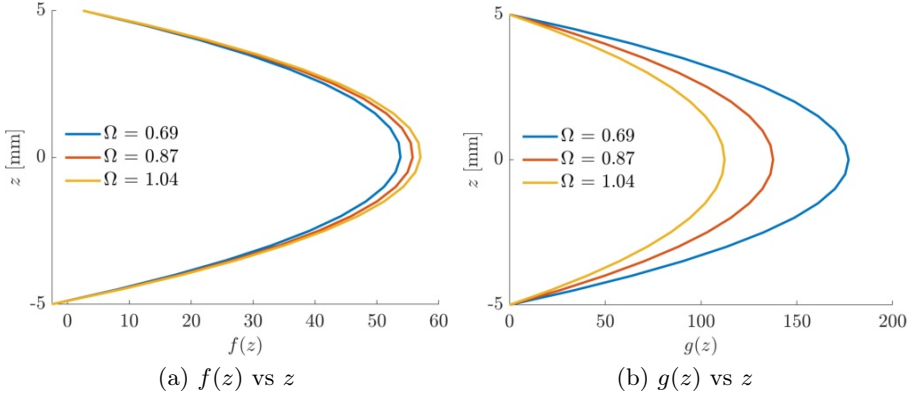


FIG. 7. Parameters $a = 5$ mm, $h = 5$ mm, $\alpha_2 = \alpha_4 = 2$, $\alpha_3 = \alpha_5 = 1$, $\beta_2 = -10$, $\gamma_2 = -1$, $E_1 = 0$, $E_2 = 1$, $E_3 = 0$.

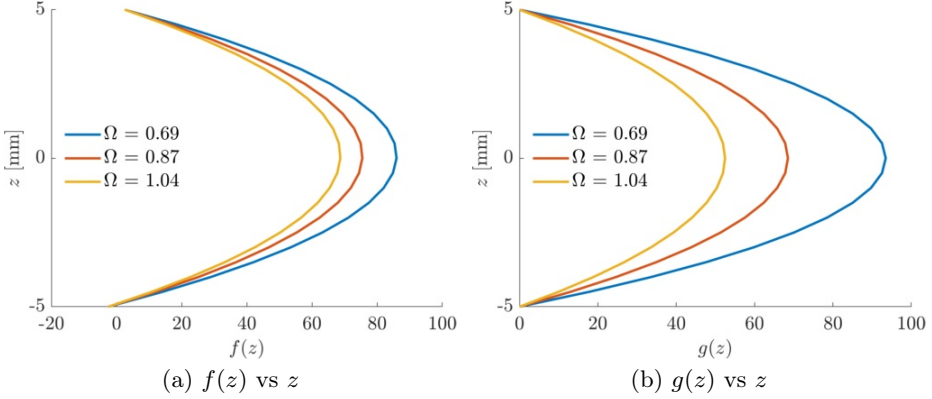


FIG. 8. Parameters $a = 5$ mm, $h = 5$ mm, $\alpha_2 = \alpha_4 = 2$, $\alpha_3 = \alpha_5 = 1$, $\beta_2 = -10$, $\gamma_2 = -1$, $E_1 = 1$, $E_2 = 1$, $E_3 = 0$.

made of the same. Also, it is assumed that a constant electric field can be enforced. In reality, one has to solve Maxwell's equations in conjunction with the usual balance laws of mechanics. In fact, in practical situations, the problem has to be cast within a fully thermodynamic setting, ensuring that the second law of thermodynamics is met. This would lead to restrictions on the values that the material constants can take. Thus, this attempt is merely a first crude stab at a very complex problem.

Acknowledgements

This paper is dedicated to the memory of K. R. Rajagopal, whose contributions to many areas in continuum mechanics are numerous and significant.

References

1. T. VON KARMAN, *Über laminare und turbulente Reibung*, ZAMM – Journal of Applied Mathematics and Mechanics, **1**, 233–252, 1921.
2. G.B. BATCHELOR, *Note on a class of solutions of the Navier–Stokes equations representing rotationally symmetric flow*, Quarterly Journal of Applied Mathematics, **4**, 29–41, 1951.
3. K. STEWARTSON, *On the flow between two rotating co-axial disks*, Proceedings of the Cambridge Philosophical Society, **49**, 333–341, 1953.
4. R. BERKER, *A new solution of the Navier–Stokes equation for the motion of a fluid contained between two parallel plates rotating about the same axis*, Archiwum Mechaniki Stosowanej, **31**, 2, 265–280, 1979.
5. R. BERKER, *Integration des Equations du Mouvement d’un Fluide Visqueux, Incompressible*, Handbuch der Physik, Vol. VIII/2, Springer-Verlag, Berlin, 1963.
6. B. MAXWELL, R.P. CHARTOFF, *Studies of a polymer melt in an orthogonal rheometer*, Transactions of the Society of Rheology, **9**, 1, 41–52, 1965.
7. R.B. BIRD, E.K. HARRIS, JR., *Analysis of steady state shearing and stress relaxation in the Maxwell orthogonal rheometer*, American Institute of Chemical Engineers Journal, **14**, 5, 758–761, 1968.
8. L.L. BLYLER, JR., S.J. KURTZ, *Analysis of the Maxwell orthogonal rheometer*, Journal of Applied Polymer Science, **11**, 1, 127–131, 1967.
9. E.A. KEARSLEY, *On the flow induced by a Maxwell–Chartoff rheometer*, Journal of Research of the National Bureau of Standards, **74**, C, 19–20, 1970.
10. R.J. GORDON, W.R. SCHOWALTER, *On the relation between complex viscosity and steady state shearing in the Maxwell orthogonal rheometer*, American Institute of Chemical Engineers Journal, **16**, 2, 318–320, 1970.
11. C. GOLDSTEIN, W.R. SCHOWALTER, *Further studies of fluid nonlinearity: The orthogonal rheometer and the oscillating sphere*, Transactions of the Society of Rheology, **19**, 1, 1–19, 1975.
12. F. AHRENS, C. GOLDSTEIN, *Viscous dissipation in the flow between eccentric rotating disks (orthogonal rheometer)*, Transactions of the Society of Rheology, **21**, 2, 207–217, 1977.
13. K.R. RAJAGOPAL, *The flow of a second order fluid between rotating parallel plates*, Journal of Non-Newtonian Fluid Mechanics, **9**, 185–190, 1981.
14. K.R. RAJAGOPAL, A.S. WINEMAN, *Flow of a BKZ fluid in an orthogonal rheometer*, Journal of Rheology, **27**, 5, 509–516, 1983.
15. K.R. RAJAGOPAL, M. RENARDY, Y. RENARDY, A.S. WINEMAN, *Flow of viscoelastic fluids between plates rotating about distinct axes*, Rheologica Acta, **25**, 459–467, 1986.
16. M. BOWER, A.S. WINEMAN, K.R. RAJAGOPAL, *Flow of K-BKZ fluids between parallel plates rotating about distinct axes: Shear thinning and inertial effects*, Journal of Non-Newtonian Fluid Mechanics, **22**, 3, 289–307, 1987.
17. L. FUSI, R. TOZZI, A. FARINA, K.R. RAJAGOPAL, *Flow of a limited stress fluid between plates rotating about different axes*, Acta Mechanica, **234**, 12, 6691–6703, 2023.

18. K. YANAMUNDRA, C.C. BENJAMIN, K.R. RAJAGOPAL, *Flow of a colloidal solution in an orthogonal rheometer*, Physics of Fluids, **36**, 043334, 2024, <https://doi.org/10.1063/5.0200595>.
19. K.R. RAJAGOPAL, A.S. GUPTA, *Flow and stability of a second grade fluid between parallel plates*, Archives of Mechanics, **33**, 663–674, 1981.
20. K.R. RAJAGOPAL, *Flow of viscoelastic fluids between rotating disks*, Theoretical and Computational Fluid Dynamics, **4**, 185–206, 1992.
21. K.R. RAJAGOPAL, *On the flow of a simple fluid in an orthogonal rheometer*, Archive for Rational Mechanics and Analysis, **79**, 39–47, 1982.
22. W. NOLL, *Motions with constant stretch history*, Archive for Rational Mechanics and Analysis, **11**, 97–105, 1962.
23. R.S. RIVLIN, J.L. ERICKSEN, *Stress-deformation relations for isotropic materials*, Journal of Rational Mechanics and Analysis, **4**, 323–425, 1955.
24. W. NOLL, *A mathematical theory of the mechanical behavior of continuous media*, Archive for Rational Mechanics and Analysis, **2**, 197–226, 1958.
25. W. NOLL, *A new mathematical theory of simple materials*, Archive for Rational Mechanics and Analysis, **48**, 1–50, 1972.
26. K.R. RAJAGOPAL, A.S. WINEMAN, *New exact solutions in non-linear elasticity*, International Journal of Engineering Science, **23**, 217–234, 1985.
27. M.M. CARROLL, K.R. RAJAGOPAL, *Pseudo-planar elastic deformations and motions of non-linear elastic solids*, Special Volume in honor of Professor R. Berker's 75th Birthday, Bulletin of the Technical University of Istanbul, **27**, 317–332, 1986.
28. K.R. RAJAGOPAL, A.S. WINEMAN, *On a class of deformations of a material with non-convex stored energy functions*, Journal of Structural Mechanics, **12**, 471–482, 1984.
29. K.R. RAJAGOPAL, M. MASSOUDI, A.S. WINEMAN, *Flow of granular materials between rotating disks*, Mechanics Research Communications, **21**, 629–634, 1994.
30. K.R. RAJAGOPAL, G. GUPTA, R.C. YALAMANCHILI, *A rheometer for measuring the properties of granular materials*, Particulate Science and Technology, **18**, 39–55, 2000.
31. K.R. RAJAGOPAL, A.S. WINEMAN, *A constitutive equation for nonlinear electroactive solids*, Acta Mechanica, **135**, 219–228, 1999.
32. K.R. RAJAGOPAL, M. RUZICKA, *On the modeling of electrorheological materials*, Mechanics Research Communications, **23**, 401–407, 1996.
33. K.R. RAJAGOPAL, M. RUZICKA, *Mathematical modeling of electrorheological materials*, Continuum Mechanics and Thermodynamics, **13**, 1, 59–78, 2001.
34. R. BUSTAMANTE, K.R. RAJAGOPAL, *On a new class of electroelastic bodies: Part I*, Proceedings of the Royal Society, Series A, London, **469**, 20120521, 2013.
35. R. BUSTAMANTE, K.R. RAJAGOPAL, *On a new class of electroelastic bodies: Part 2*, Proceedings of the Royal Society, Series A, London, **489**, 20130106, 2013.
36. K.R. RAJAGOPAL, *On implicit constitutive theories*, Applications of Mathematics, **28**, 4, 279–319, 2003.

-
37. K.R. RAJAGOPAL, *Elasticity of elasticity*, Zeitschrift für Angewandte Mathematik und Physik, **58**, 309–317, 2007.
 38. K.R. RAJAGOPAL, A.S. WINEMAN, *Universal relations for electroactive solids undergoing shear and triaxial extension*, International Journal of Non-Linear Mechanics, **169**, 104954, 2025.
 39. K.R. RAJAGOPAL, A.S. WINEMAN, *New universal relations for nonlinear isotropic elastic materials*, Journal of Elasticity, **17**, 75–83, 1987.

Received December 21, 2024, revised version April 3, 2025.

Published online July 14, 2025.
